



Significance and Usefulness of the t_{ij} Concept

Teruo Nakai^(✉)

Geo-Research Institute and Chubu University, Nagoya, Japan
nakai.teruo@nitech.ac.jp

Abstract. Constitutive models formulated using the stress invariants (p and q) cannot describe uniquely the deformation and strength of geomaterials under three principal stresses [1]. Then, the concept of t_{ij} has been proposed to describe uniquely the stress-strain behaviors in general three-dimensional (3D) stress conditions [2]. This concept was found out from the idea that the frictional law essentially governs soil behavior. Since the formulation of elastoplastic model using this concept was described in the previous papers [3, 4], the meaning of this concept and its usefulness are presented in this paper.

Keywords: Constitutive modeling · Spatially mobilized plane · Concept of t_{ij}

1 Stress Invariants in 2D Condition

Figure 1 shows the Mohr's stress circle on τ - σ plane in two-dimensional (2D) condition. Now, 2D soil models are usually formulated using the normal stress $\sigma_{45^\circ}(=s)$ and shear stress $\tau_{45^\circ}(=t)$ on the plane where shear stress is maximized (called τ_{\max} plane or 45° plane). On the other hand, Murayama [5] paid his attention not to this plane but to the plane where the shear normal stress ratio is maximized (called $(\tau/\sigma_N)_{\max}$ plane or mobilized plane), because it is considered appropriate that soil behavior during shear is governed by the frictional law. The shear normal stress ratios on these planes are expressed as follows:

$$\frac{\tau_{45^\circ}}{\sigma_{45^\circ}} = \frac{t}{s} = \sin \phi_{mo} = \frac{\sigma_1 - \sigma_3}{\sigma_1 + \sigma_3} \quad (1)$$

$$\frac{\tau}{\sigma_N} = \tan \phi_{mo} = \frac{\sigma_1 - \sigma_3}{2\sqrt{\sigma_1 \sigma_3}} \quad (2)$$

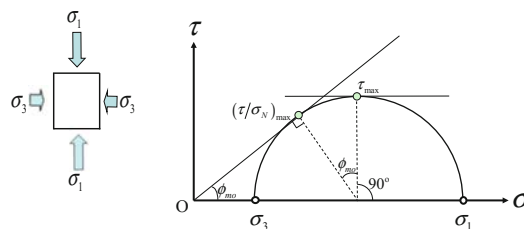


Fig. 1. Two reference planes (τ_{\max} plane and $(\tau/\sigma_N)_{\max}$ plane) expressed on Mohr's stress circle

It is noticed that when the principal stress ratio σ_1/σ_3 changes from 1 to infinite (the mobilized angle ϕ_{mo} changes from 0° to 90°), the stress ratio τ/σ_N in Eq. (2) can take a value of 0 to infinite, but the value of stress ratio $\tau_{45^\circ}/\sigma_{45^\circ}$ expressed by Eq. (1) should be between 0 and 1. Although 2D model can be formulated using stress invariants, it is necessary that the stress ratio $\tau_{45^\circ}/\sigma_{45^\circ}(=t/s)$ is less than 1 when the model is formulated by the stresses on 45° plane.

2 Octahedral Plane and Spatially Mobilized Plane

In 3D condition, three Mohr's stress circles between respective two principal stresses can be drawn. So, there are three 45° planes on which the shear stresses are maximized between two principal stresses as shown in Fig. 2(a). The plane where these three 45° planes are combined is called the octahedral plane, which has been usually employed as the reference plane in constitutive modeling of metals and geomaterials [1]. On the other hand, three mobilized planes where shear normal stress ratio is maximized between respective two principal stresses are also described as shown in Fig. 2(b). The specially mobilized plane (SMP) is defined as the combined plane of these three mobilized planes [6]. Although the direction cosines of octahedral plane are given by $(1/\sqrt{3}, 1/\sqrt{3}, 1/\sqrt{3})$, the direction cosines of SMP are given as a function of stress ratio by

$$(a_1, a_2, a_3) = \left(\sqrt{I_3/(I_2\sigma_1)}, \sqrt{I_3/(I_2\sigma_2)}, \sqrt{I_3/(I_2\sigma_3)} \right) \quad (3)$$

Here, I_2 and I_3 are the second and third invariants of the Cauchy stress σ_{ij} . Also, the unit symmetric tensor, a_{ij} , whose principal values are given by these direction cosines, can be defined.

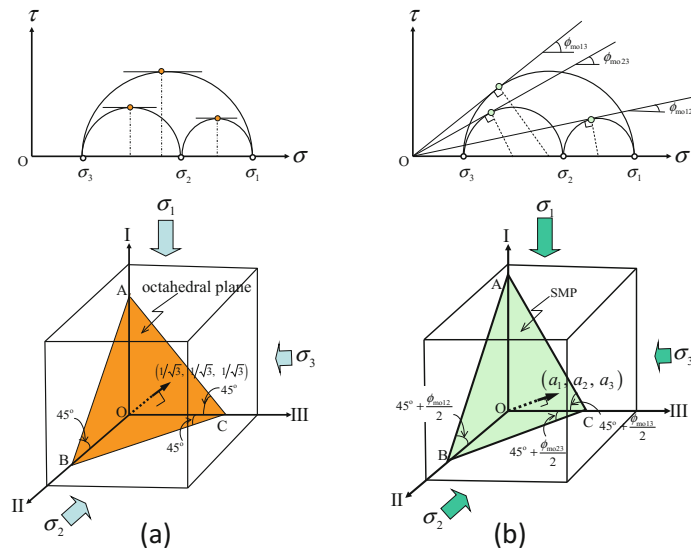


Fig. 2. (a) Octahedral plane and (b) Spatially mobilized plane (SMP)

3 Formulation of 3D Elastoplastic Models

3.1 Ordinary Modeling Using Stress Invariants (p and q) [1]

The mean stress p and the deviatoric stress q correspond to the normal and in-plane components of the stress with respect to the octahedral plane as shown in Fig. 3, and are expressed by Eq. (4) using three principal stresses.

$$\begin{cases} p = \sqrt{\frac{1}{3}}ON = \frac{1}{3}(\sigma_1 + \sigma_2 + \sigma_3) = \sigma_{oct} \\ q = \sqrt{\frac{3}{2}}NP = \frac{1}{\sqrt{2}}\sqrt{(\sigma_1 - \sigma_2)^2 + (\sigma_2 - \sigma_3)^2 + (\sigma_3 - \sigma_1)^2} = \frac{3}{\sqrt{2}}\tau_{oct} \end{cases} \quad (4)$$

The yield function (plastic potential) $f=0$ is formulated using these stress invariants, and the plastic strain increments is calculated assuming flow rule (normality condition) in the Cauchy stress σ_{ij} .

$$d\epsilon_{ij}^p = \Lambda \frac{\partial f}{\partial \sigma_{ij}} = \Lambda \left(\frac{\partial f}{\partial p} \frac{\partial p}{\partial \sigma_{ij}} + \frac{\partial f}{\partial \eta} \frac{\partial \eta}{\partial \sigma_{ij}} \right) \quad (\text{where } \eta=q/p) \quad (5)$$

Figure 4 shows the yield surface and normality rule in (p, q) plane under triaxial compression ($\sigma_1 > \sigma_2 = \sigma_3$; upper half) and triaxial extension ($\sigma_1 = \sigma_2 > \sigma_3$; lower half). The yield surface is symmetric with respect to p -axis. Also, stress condition without tension stress is limited in gray color area. Then, some normal stress becomes negative when stress ratio q/p becomes larger than the broken lines ($\sigma_3 = 0$) during elastic deformation or elastoplastic deformation, even if p is positive.

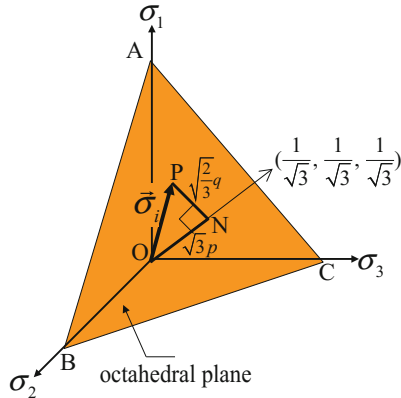


Fig. 3. Definitions of (p and q)

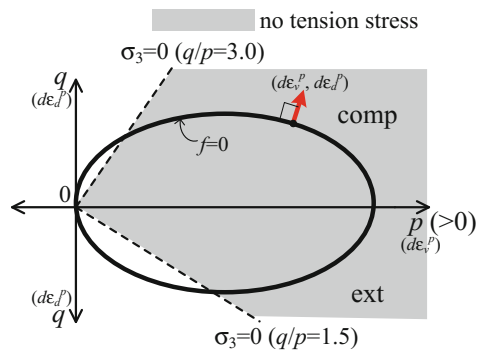


Fig. 4. Yield surface on p - q plane and no tension area

3.2 Modeling Based on t_{ij} Concept [2]

The modified stress tensor t_{ij} is defined by the product of a_{ik} and σ_{kj} as follows:

$$t_{ij} = a_{ik}\sigma_{kj} \quad (6)$$

Its principal values are given by

$$t_1 = a_1\sigma_1, \quad t_2 = a_2\sigma_2, \quad t_3 = a_3\sigma_3 \quad (7)$$

The invariants of modified stress (t_N and t_S) used in t_{ij} concept are defined as the normal and in-plane components of t_{ij} to the SMP as shown in Fig. 5.

$$\begin{cases} t_N = ON = t_1a_1 + t_2a_2 + t_3a_3 = 3I_3/I_2 \\ t_S = NT = \sqrt{(t_1a_2 - t_2a_1)^2 + (t_2a_3 - t_3a_2)^2 + (t_3a_1 - t_1a_3)^2} \end{cases} \quad (8)$$

The yield function $f = 0$ based on the t_{ij} concept is formulated using the stress invariants (t_N and t_S) instead of (p and q).

$$de_{ij}^p = \Lambda \frac{\partial f}{\partial t_{ij}} = \Lambda \left(\frac{\partial f}{\partial t_N} \frac{\partial t_N}{\partial t_{ij}} + \frac{\partial f}{\partial X} \frac{\partial X}{\partial t_{ij}} \right) \quad (\text{where } X = t_S/t_N) \quad (9)$$

Figure 6 shows schematically the yield surface in $t_N - t_S$ plane under triaxial compression (upper half) and triaxial extension (lower half) in the same way as Fig. 4. The yield surface is symmetric with respect to the t_N -axis. The area where tension stress does not occur is indicated by gray color area, because σ_3 is always positive in case of $t_N > 0$ (see Eq. (8)). Also, there is no tension zone inside of the yield surface. This is because $\sigma_3 = 0$ condition is satisfied on the vertical axis (t_S axis) in Fig. 6.

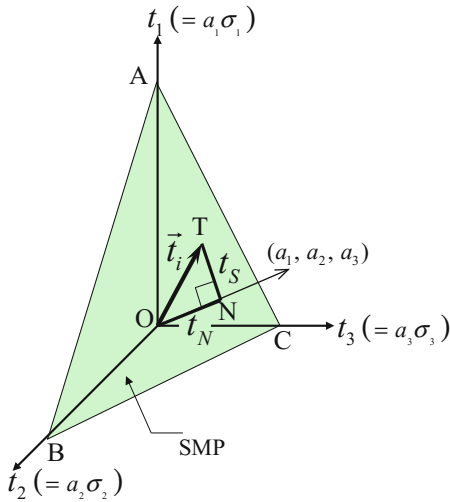


Fig. 5. Definitions of (t_N and t_S)

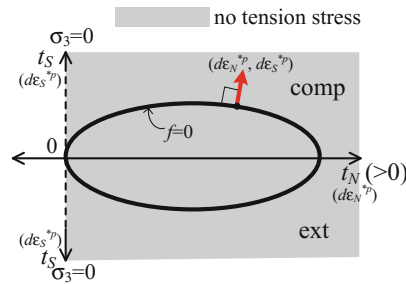


Fig. 6. Yield surface on $t_N - t_S$ plane and no tension area

4 Meaning of t_{ij} Concept

From microscopic observation, Oda [7] showed that, as the stress ratio increases, the average directions normal to the inter-particle contacts gradually concentrate in the same direction as the major principal stress (σ_1). Satake [8] pointed out that the principal values (φ_1, φ_2) of the so-called fabric tensor φ_{ij} , which represents the relative distribution of the number of vectors normal to the inter-particle contacts, is approximately proportional to the square root of the corresponding principal stresses.

$$\frac{\varphi_1}{\varphi_2} \approx \left(\frac{\sigma_1}{\sigma_2} \right)^{0.5} \quad (10)$$

Employing a fabric tensor, Satake [9] also proposed a modified stress tensor σ_{ij}^*

$$\sigma_{ij}^* = \frac{1}{3} \varphi_{ik}^{-1} \sigma_{kj} \quad (11)$$

Figure 7(a) shows schematically the distribution of inter-particle contacts in 2D condition. Considering an equivalent continuum, such material exhibits anisotropy since the stiffness in the σ_1 direction should be larger than that in the σ_2 direction with the increase of stress ratio (see diagram (b)). When adopting an elastoplastic theory, it is reasonable to treat the soil as an isotropic material by introducing the modified stress t_{ij} in which induced anisotropy is already considered. This is because the normality rule should hold in the isotropic space, like the transformed space used to analyze seepage problems in anisotropic ground and others. From Eq. (3), the principal values of a_{ij} are inversely proportional to the square root of the principal stresses, therefore:

$$a_1 : a_2 = 1/\sqrt{\sigma_1} : 1/\sqrt{\sigma_2} \quad (12)$$

It can be noted that a_{ij} corresponds to the inverse of the fabric tensor in Eq. (10), and t_{ij} defined by Eq. (6) corresponds to the modified stress in Eq. (11). As shown in diagram (c), the stress ratio t_1/t_2 in the modified stress space is smaller than stress ratio σ_1/σ_2 in the ordinary stress space. Then, it is reasonable to assume that the flow rule (normality condition) holds not in the σ_{ij} space but in the t_{ij} space, because the

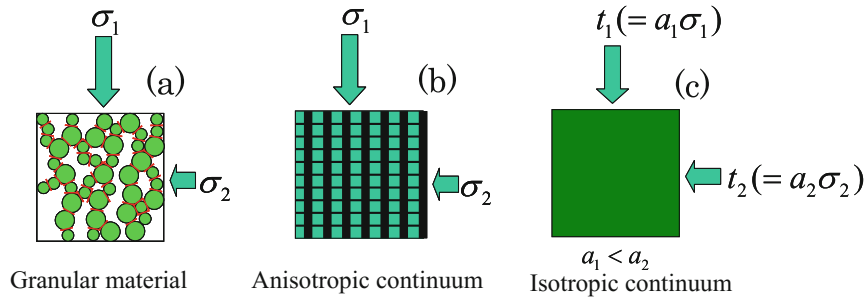


Fig. 7. Induced anisotropy during shear loading and meaning of t_{ij} concept

condition of the anisotropic material in diagram (b) can be considered to be the same as that of the isotropic material in diagram (c).

5 Verification by Test Data

Figure 8 shows the observed results (dots) of drained triaxial compression and extension tests on normally consolidated clay and the corresponding calculated results (curves) based on t_{ij} concept. Although models using (p, q) invariants cannot describe the difference between triaxial compression and extension tests, the model based on t_{ij} concept describes well the observed results. The unique relation between d_N^*/d_S^* and t_S/t_N in Fig. 9, which is independent of intermediate principal stress, means that the shape of yield surface is symmetric with respect to t_N axis as shown in Fig. 6. Figure 10 shows the observed and calculated directions of the shear strain increments on the octahedral plane for true triaxial ($\sigma_1 > \sigma_2 > \sigma_3$) tests. The calculated directions

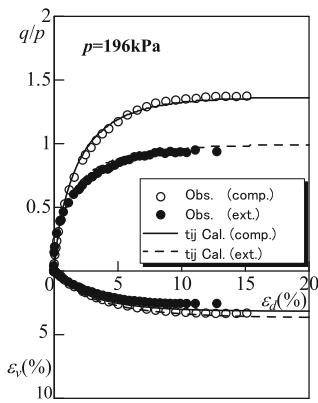


Fig. 8. Stress-strain relation

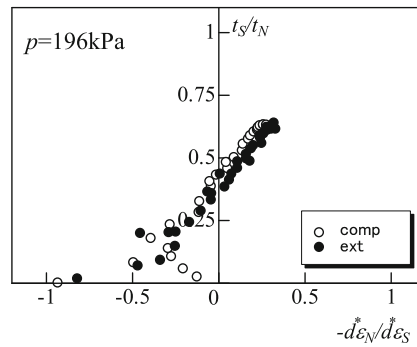


Fig. 9. Observed stress-dilatancy relation

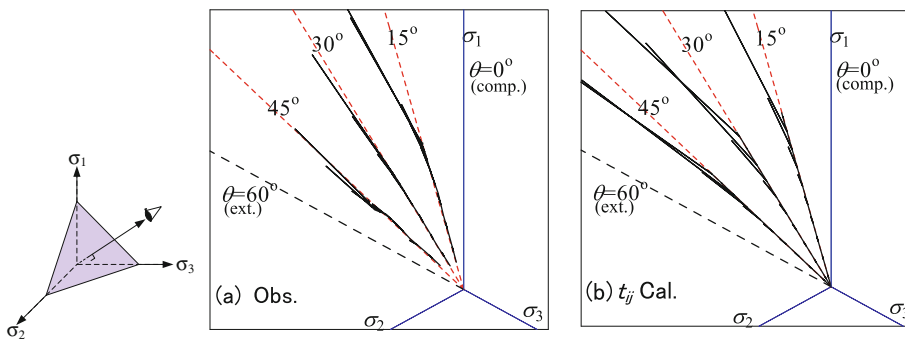


Fig. 10. Observed and calculated directions of shear strain increment on octahedral plane

describe well the observed tendency that the direction of the shear strain increments deviates leftward from that of shear stress (radial direction) with the increase in stress ratio under three different principal stresses. On the other hand, the calculated directions by ordinary (p, q) model are always radial.

References

1. Schofield, A.N., Wroth, C.P.: Critical State Soil Mechanics. McGraw-Hill, London (1968)
2. Nakai, T., Mihara, Y.: A new mechanical quantity for soils and its application to elastoplastic constitutive models. *Soils Found.* **24**(2), 82–94 (1984)
3. Nakai, T., Hinokio, T.: A simple elastoplastic model for normally and over consolidated soils with unified material parameters. *Soils Found.* **44**(2), 53–70 (2004)
4. Nakai, T.: Constitutive Modeling of Geomaterials: Principles and Applications. CRC Press, Boca Raton (2012)
5. Murayama, S.: A theoretical consideration on a behavior of sand. In: Proceedings of IUTAM Symposium on Rheology and Soil Mechanics, Grenoble, pp. 146–159 (1964)
6. Matsuoka, H., Nakai, T.: Stress-deformation and strength characteristics of soil under three different principal stresses. *Proc. JSCE* **232**, 59–70 (1974)
7. Oda, M.: The mechanism of fabric changes during compressional deformation of sand. *Soils Found.* **12**(2), 1–18 (1972)
8. Satake, M.: Anisotropy in ground and soil materials. *Tsuchi Kiso* **32**(11), 5–12 (1984, in Japanese)
9. Satake, M.: Fabric tensor in granular materials. In: Proceedings of IUTAM Conference on Deformation and Failure of Granular Materials, Delft, pp. 63–68 (1982)